ORGANIC CHEMISTRY FRONTIERS

RESEARCH ARTICLE

View Article Online
View Journal | View Issue



Cite this: *Org. Chem. Front.*, 2025, **12**, 1432

# A persistent concealed non-Kekulé nanographene: synthesis and *in situ* characterization†

Muhammad Imran, ‡[a,b] Lin Yang,‡[a,b] Jin-Jiang Zhang,[b] Zhen-Lin Qiu,[a] Yubin Fu, [a,b] Noel Israel, [c] Evgenia Dmitrieva, [c] Andrea Lucotti, [d] Gianluca Serra,[d] Matteo Tommasini, [d] Ji Ma *[e] and Xinliang Feng *[a,b]

Received 29th October 2024,
Accepted 18th December 2024

DOI: 10.1039/d4qo02019g

rsc.li/frontiers-organic

Concealed non-Kekulé (CNK) nanographenes have recently gained attention as promising non-Kekulé model systems due to their distinctive antiferromagnetic electronic spins, which offer potential applications in spintronics and quantum information science. However, synthesizing CNK nanographenes in solution remains a significant challenge because of their strong biradical character and high reactivity. In this study, we report the successful synthesis of a novel CNK nanographene with two phenalene units fused in a *cis* configuration to perylene (**c-CNK**), which exhibits persistent stability under ambient conditions, with a half-life ($t_{1/2}$) of 59 minutes. The formation of **c-CNK** is confirmed using *in situ* UV-Vis-NIR spectroscopy, Raman spectroscopy, and high-resolution mass spectrometry. The open-shell character of **c-CNK** is supported by electron paramagnetic resonance (EPR) spectroscopy by observing an isotropic signal with a *g*-value of 2.0026. Quantum chemical simulations reveal a high biradical character ($y_0$ = 0.97) and a singlet open-shell ground state with a small singlet–triplet energy gap ($\Delta E_{S-T}$) of 0.4 kcal mol$^{-1}$. This work presents a solution synthesis of a next-generation concealed non-Kekulé nanographene with intrinsic antiferromagnetic electronic spins, highlighting its potential as a promising material for future quantum technologies.



## Introduction

π-Magnetism in fused polycyclic hydrocarbons, commonly known as nanographenes (NGs), has recently attracted significant attention in various scientific fields including chemistry, condensed matter physics, and materials science.[1–11] Among them, non-Kekulé NGs are particularly interesting owing to their unique arrangement of π-electrons such that a Kekulé structure is impossible without leaving unpaired electron(s).[12] Phenalene, composed of three fused benzene rings, is the smallest non-Kekulé NG and has been extensively studied since its first isolation in crystalline form back in 1999 by Kubo.[13] However, large members of the non-Kekulé family have remained elusive due to their high reactivity even at low temperatures resulting in air oxidation or sigma dimerization.[14] In a recent work,[3] triangulene derivatives have been achieved both *in situ* and in the crystalline form separately through solution synthesis by sufficient steric protection enabling kinetic stability.[15,16] Overall, less effort has been directed towards the solution synthesis of non-Kekulé NGs, owing to the challenges in isolation and purification along with high risks of air oxidation or decomposition of these hard-earned final π-magnetic molecules.

Non-Kekulé NGs can be categorized into (i) obvious non-Kekulé NGs and (ii) concealed non-Kekulé NGs based on the difference in their sublattice and net spin in their lowest energy ground state. In contrast to the obvious non-Kekulé NGs, concealed non-Kekulé NGs (CNKs) have two unpaired electronic spins aligned anti-parallel (anti-ferromagnetic) to each other in the ground state (Fig. 1). The topological frustration of π-bonds in a CNK renders it impossible to assign a classical Kekulé structure without leaving unpaired electrons, driving the system into a magnetically non-trivial open-shell ground state.[17–19] CNK-NGs mostly remained an interesting subject of mathematical chemistry owing to their structural peculiarity.[20] For example, the smallest CNK can be possible in

[a]*Center for Advancing Electronics Dresden (cfaed) & Faculty of Chemistry and Food Chemistry, Technische Universität Dresden, 01062 Dresden, Germany. E-mail: xinliang.feng@tu-dresden.de*
[b]*Max Planck Institute of Microstructure Physics Weinberg 2, 06120 Halle, Germany*
[c]*Leibniz Institute for Solid State and Materials Research, 01069 Dresden, Germany*
[d]*Dipartimento di Chimica, Materiali e Ingegneria Chimica "G. Natta", Politecnico di Milano, Piazza Leonardo da Vinci 32, 20133 Milano, Italy*
[e]*College of Materials Science and Opto-Electronic Technology & Center of Materials Science and Optoelectronics Engineering, University of Chinese Academy of Science, 100049 Beijing, P. R. China. E-mail: maji@ucas.ac.cn*

†Electronic supplementary information (ESI) available. CCDC 2390595. For ESI and crystallographic data in CIF or other electronic format see DOI: https://doi.org/10.1039/d4qo02019g

‡These authors contributed equally to this work.

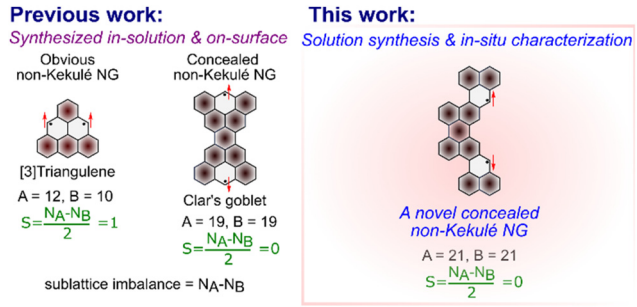


**Fig. 1** Previous work on non-Kekulé NGs. The concealed non-Kekulé NG has only been achieved *via* on-surface-assisted synthesis and the current work represents the first synthesis of a CNK in solution and *in situ* characterization.

a special arrangement of eleven fused benzene rings, resulting in only 8 possible arrangements.

Early synthetic efforts towards CNK-NGs by Eric Clar date back to 1972 which resulted in the unsuccessful realization of targeted molecules.[21] The representative bow-tie-shaped CNK-NG known as Clar's Goblet was successfully achieved by our group in 2020 in collaboration with Fasel *et al.*, through a combined in-solution and on-surface synthesis approach.[22] The discovery of antiferromagnetically coupled spins in a CNK (Clar's Goblet), with an effective exchange parameter ($J_{\mathrm{eff}}$) of 23 meV, exceeding the dissipation limit, has sparked interest in their potential for fault-tolerant spin-logic operations near room temperature for quantum computing technologies. Surface-assisted synthesis has undoubtedly become a promising alternative for producing challenging molecular systems like non-Kekulé NGs.[4,23–28] However, this approach encounters several fundamental limitations, including low yield, poor selectivity, limited scalability, and the necessity for a planar structure. As a result, there is an increasing need to develop robust solution synthesis methods and design structures that offer both scalability and enhanced stability.

Herein, we report the solution synthesis of a novel nonplanar CNK nanographene named **c-CNK** with very high biradical character ($y_0$ = 0.97) by building two phenalene units in a *cis* configuration at the 3,10-positions of the perylene core through multi-step synthesis (Fig. 1). The key precursor **2H-c-CNK** is achieved by the installation of naphthalene with a benzylic ester functionality at the 3,10-positions of dibromoperylene *via* double Suzuki–Miyaura coupling. The final **c-CNK** is synthesized through oxidative dehydrogenation of the key precursor **2H-c-CNK** by treatment with tetrachloro-1,4-benzoquinone (TCBQ). The two mesityl substituents at high spin positions of the CNK provide optimum steric protection, ensuring a reasonable stability with a half-life ($t_{1/2}$) of 59 min in solution under ambient conditions. The *in situ* formation of **c-CNK** is confirmed by UV-Vis-NIR spectroscopy, high-resolution (HR) matrix-assisted laser desorption/ionization time-of-flight (MALDI-TOF) mass spectrometry and Raman spectroscopy. **c-CNK** shows a narrow optical energy gap ($E_{\mathrm{opt.}}$) of 1.07 eV as revealed by UV-Vis-NIR absorption data. The open-shell character of **c-CNK** is supported by electron paramagnetic resonance (EPR) spectroscopy. This study provides a synthetic approach for accomplishing novel CNK systems where two spins are anti-ferromagnetically coupled in a single molecule in the ground state.

## Results and discussion

To realize the synthesis of **c-CNK**, we conceived a synthetic route as illustrated in Scheme 1. Firstly, the initial precursor **4** was synthesized *via* 4-step synthesis by using commercially available 1,8-dibromonaphthalene as the starting material. Compound **1** was synthesized by selective lithiation using *n*-BuLi followed by electrophilic addition of methyl iodide at low temperature. Next, benzylic bromination was performed on **1** using *N*-bromosuccinimide in carbon tetrachloride solvent at 80 °C to achieve compound **2**.

Subsequently, compound **2** was reacted with potassium acetate at 100 °C to obtain **3**. Finally, palladium catalyzed borylation was performed on **3** to get the precursor **4** with a boronic ester functionality for subsequent double Suzuki–Miyaura coupling with 3,10-dibromoperylene. Next, the key precursor **2H-c-CNK** was achieved in four steps. After successful double Suzuki–Miyaura coupling, 3,10-dibromoperylene afforded compound **5** with a benzylic ester functionality which was subjected to hydroxylation with KOH without further purification to afford compound **6** in 72% yield over two steps. Compound **6** was oxidized by Dess–Martin oxidation to obtain compound **7** in 41% yield. Afterward, compound **7** was treated with an excess of 2-mesitylmagnesium bromide to produce the diol *in situ*, which was then subjected to Friedel–Crafts alkylation promoted by $BF_3{\cdot}OEt_2$ to afford the dihydro-precursor **2H-c-CNK** with a yield of 68% in two steps. Notably, the key precursor **2H-c-CNK** was confirmed by single crystal X-ray diffraction (XRD) analysis, MALDI-TOF, and NMR spectroscopy (Fig. S4†). All of the intermediates were purified and fully characterized by HR MALDI-TOF mass spectrometry and NMR ($^1$H and $^{13}$C) spectroscopy.

We further monitored the oxidative dehydrogenation reaction of the precursor **2H-c-CNK** using different oxidation conditions. The most successful results were obtained when tetrachloro-1,4-benzoquinone (TCBQ) was used as an oxidant in a toluene solution of **2H-c-CNK** at 100 °C as evident from UV-Vis-NIR spectroscopy and MALDI-TOF mass analysis of the reaction mixture. HR MALDI-TOF mass analysis of the reaction mixture in positive mode revealed that the intense signal at $m/z$ = 764.3451 of the precursor **2H-c-CNK** ([$M^+$]), calculated for $C_{64}H_{44}$ as 764.3443, disappeared and a new signal emerged at $m/z$ = 762.3288 (Scheme 1), which is fully consistent with the expected molecular mass of **c-CNK** ([$M^+$]), calculated for $C_{64}H_{42}$ as 762.3281, validating the successful formation of the targeted **c-CNK**. Notably, the isotopic distribution observed for the obtained **c-CNK** agrees with the simulated pattern for $C_{64}H_{42}$. Due to the high biradical character and high reactivity of **c-CNK**, conventional structural characterization by NMR

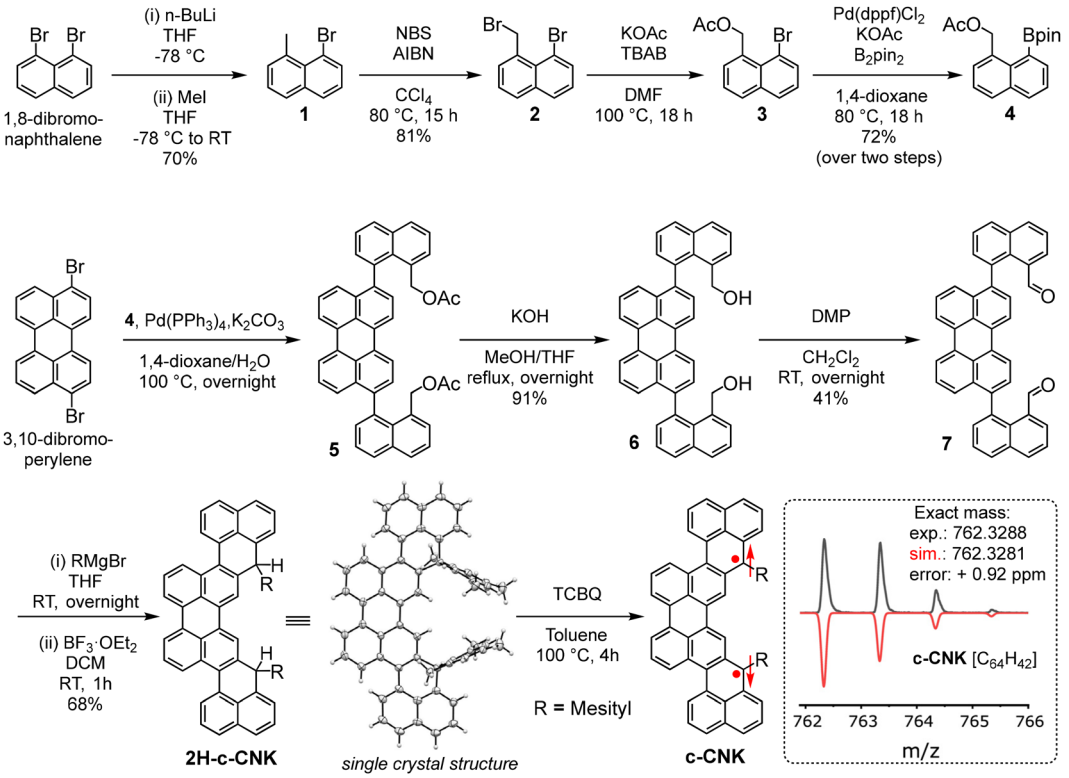


**Scheme 1** Synthesis of **2H-c-CNK** and **c-CNK**. NBS (*N*-bromosuccinimide); AIBN (azobisisobutyronitrile); TBAB (tetrabutylammonium bromide); DMP (Dess–Martin periodinane); TCBQ (tetrachloro-1,4-benzoquinone).

spectroscopy and single-crystal structural analysis or attempts to isolate and purify **c-CNK** did not succeed. Therefore, we turned to *in situ* UV-Vis-NIR spectroscopy which is a powerful tool to characterize open-shell NGs due to the characteristic low energy absorption bands in the NIR region associated with SOMO to LUMO transitions. As shown in Fig. 2a, the dihydro-precursor **2H-c-CNK** only shows UV-Vis absorption below $\lambda$ = 560 nm. In contrast, the UV-Vis-NIR absorption spectrum of **c-CNK** displays the characteristic low-energy absorption bands with absorption wavelengths ($\lambda$) extending up to 1150 nm resulting from electronic excitation from SOMO to LUMO with vibronic features related to absorption bands at 940 nm, 866 nm, 809 nm, and 727 nm. A narrow optical energy gap ($E_{opt.}$) of 1.07 eV is revealed by UV-Vis-NIR absorption data of **c-CNK**. The spectral changes accompanied by colour changes from yellow to greenish-brown can obviously be attributed to the *in situ* formation of **c-CNK**.

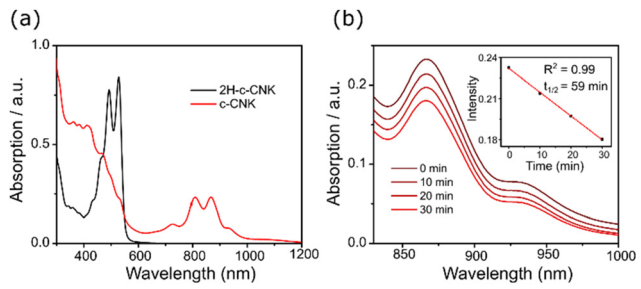


**Fig. 2** (a) UV-Vis-NIR absorption spectra of compounds **2H-c-CNK** and **c-CNK**. **c-CNK** displays the characteristic NIR absorption bands from SOMO to LUMO transitions, whereas **2H-c-CNK** only shows light absorption below 560 nm. (b) Time-dependent UV-Vis-NIR absorption spectra of compound **c-CNK** showing a decrease in signal intensity in the NIR region under ambient conditions.

The *in situ* generated **c-CNK** was persistent in solution under ambient conditions, as shown in Fig. 2b. Time-depended UV-Vis-NIR absorption spectra of **c-CNK** were obtained to test its stability. The spectroscopic results reveal that the intensity of the NIR absorption bands diminishes with the concomitant increase of the peaks in the visible region suggesting the possible oxidative degradation of **c-CNK**. During the stability test, the solution of compound **c-CNK** in dry dichloromethane was exposed to ambient air and light. By plotting the change in absorption intensity with the exposure time of ambient conditions, according to the linear regression and extrapolation to % change = 0.50, the half-life time ($t_{1/2}$) of **c-CNK** was estimated to be 59 min.

Next, EPR spectroscopy was used to examine the paramagnetic nature of **c-CNK** first at 293 K. The open-shell character of **c-CNK** is supported by observing a strong isotropic signal with a *g*-value of 2.0026 in the EPR spectrum in deuterated dichloromethane (Fig. 3a). The isotropic EPR signal arises from efficient spin delocalization and weak spin–spin coupling, as further supported by DFT calculations. We further performed

 

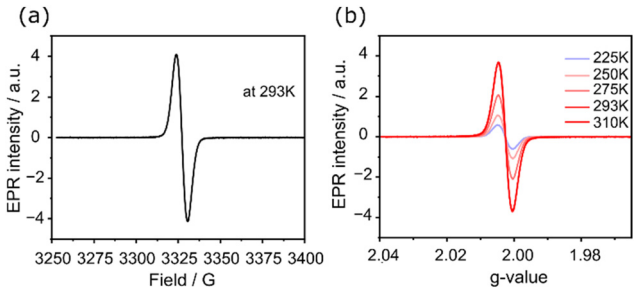


**Fig. 3** (a) EPR spectrum of **c-CNK** measured at 293 K in *d*-dichloromethane solution. (b) Variable temperature EPR spectra of **c-CNK** in *d*-dichloromethane solution.

variable-temperature EPR measurements, which show an increase in the signal intensity by increasing the temperature from 225 to 310 K (Fig. 3b and S2a†). This behaviour is typical of singlet biradicals and is the result of the thermal population of triplet states due to a smaller singlet–triplet energy gap.[29] In addition, at low temperatures, intermolecular interactions within the perylene framework lead to enhanced π–π stacking, resulting in singlet state formation due to spin–spin coupling between the interacting molecules resulting in pronounced decrease in the EPR signal.[30] The radical is not stable at high temperatures and the EPR signal intensity decreases over time (Fig. S2b†); the latter is in agreement with time-dependent UV-Vis-NIR spectroscopic measurements. Overall, these results confirm the singlet biradical character of the **c-CNK** generated *in situ* in dichloromethane solution.

To further support the successful synthesis of **c-CNK**, we measured the Raman spectra, which is also an important tool for *in situ* investigation of redox reactions in NGs.[31] We compared the experimental results with DFT calculation outcomes, as shown in Fig. 4a. The best experimental conditions for Raman spectroscopy of these compounds were reached with the excitation wavelength of 405 nm. Based on the UV-Vis-NIR absorption spectra of **2H-c-CNK** and **c-CNK** (Fig. 2a), the excitation at 405 nm wavelength yields resonance Raman conditions. In the DFT calculation of the resonance Raman spectra of **c-CNK** and **2H-c-CNK**, we obtain the best agreement with the experiments considering excitation wavelengths in the range of 405–415 nm (Fig. S3†). Understandably, these values are not identical to the experimental excitation wavelength (405 nm) because of the differences between the local molecular conditions of the sample and those of the isolated molecular model, which lacks intermolecular interactions and crystal packing effects. Nevertheless, all the spectra show good agreement with their computational counterparts. The precursor **2H-c-CNK** and the *in situ* generated **c-CNK** were analyzed with excitation at 405 nm. For the precursor **2H-c-CNK**, the experimental Raman bands at 1357 and 1383 $cm^{-1}$ are assigned to the collective CC stretching modes of the graphene moiety. We also assign the intense feature at 1582 $cm^{-1}$, as well as the shoulder at 1607 $cm^{-1}$, to G modes. In the spectrum of **c-CNK**, we assign the band at 1383 $cm^{-1}$ to collective

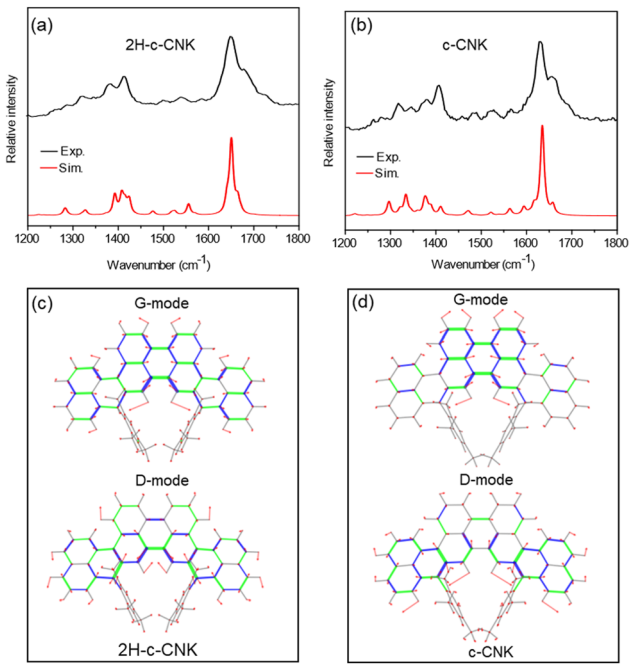


**Fig. 4** Top panel: experimental (black lines) and simulated (red lines) Raman spectra of (a) **2H-c-CNK** and (b) **c-CNK**. Each spectrum has been normalized to unity. The simulated spectrum of **2H-c-CNK** was computed with 410 nm excitation and that of **c-CNK** with 406 nm excitation resonance. Bottom panel: representation of the nuclear displacements assigned to the strongest G and D peaks observed in the experimental spectra of (c) **2H-c-CNK** and (d) **c-CNK**; the green and blue segments represent stretching and contracting bonds, respectively, and the red lines represent nuclear displacement vectors (see the starred modes in Tables S1 and S2† for details).

CC stretching in the phenalene moiety and the peak at 1582 $cm^{-1}$, together with its shoulder at 1607 $cm^{-1}$, to the G mode of the perylene moiety. It is remarkable that the positions of the strongest features in the Raman spectrum of **2H-c-CNK** and **c-CNK** do not differ much, in agreement with DFT results. Indeed, the analysis of the nuclear displacements of the strongest modes in the G and D regions reveals similar displacement patterns in the two molecules, irrespective of the dehydrogenation. The presence/absence of the two hydrogen atoms in **2H-c-CNK** and **c-CNK**, respectively, has a weak influence on the collective vibrational dynamics of these CC stretching modes.

Quantum chemical simulations were performed to gain a deeper understanding of the electronic structure of **c-CNK**. DFT calculations were performed using the Gaussian 09 package. The geometry of the CNK was relaxed at the UB3LYP/6-311G level of theory. The DFT-optimized structures of compound **c-CNK** have a slightly curved backbone geometry with the mesityl substitutions perpendicular to the core structure (Fig. 5a). A comparison of the optimized singlet and triplet ground states of **c-CNK** shows that the singlet state, where the two electronic spins are antiparallel, is the most stable state. The calculated singlet–triplet energy gap ($\Delta E_{ST}$) is small with a value of −0.42 kcal $mol^{-1}$. The biradical character ($y_0$) was

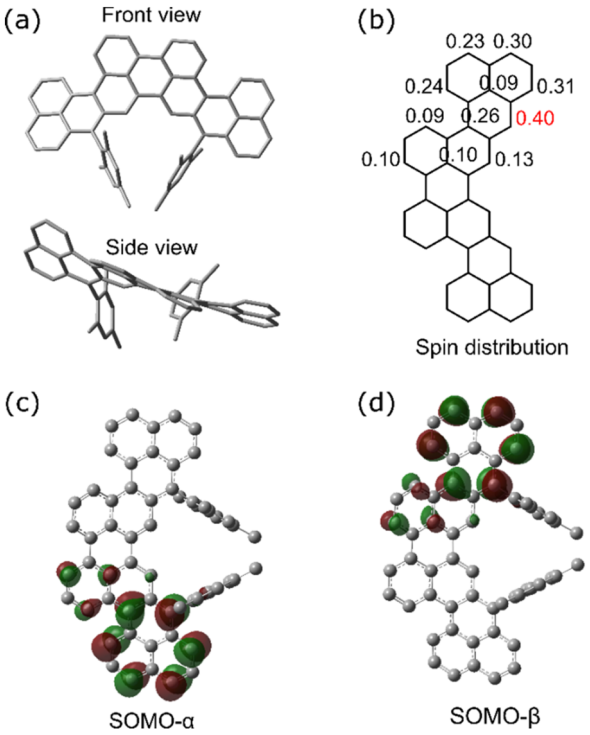


**Fig. 5** Calculation results of **c-CNK** (hydrogen atoms omitted for clarity). DFT-optimized structures of **c-CNK** at the UB3LYP/6-31G (d) level: (a) front view, and side view, (b) spin density distribution (c) SOMO-α and (d) SOMO-β.

calculated using UB3LYP/6-31G, according to the occupation numbers of the lowest singly occupied natural orbitals (SOMO) and lowest singly unoccupied natural orbitals (LUMO). The calculated high biradical yield ($y_0$) of 0.97 agrees with the non-Kekulé structure with two unpaired spins.[32] Furthermore, the spin density distribution of **c-CNK** reveals that spin is mostly concentrated over the phenalene units with the high spin density at the carbon centers attached to the mesityl-substituents (Fig. 5b). The calculated singly occupied molecular orbital (SOMO) profiles of the α and β electrons are separated from each other (Fig. 5c and d), which is typical of open-shell NGs.

## Conclusions

In summary, we have successfully synthesized a next-generation persistent concealed non-Kekulé NG *via* multi-step solution synthesis. The synthesis of **c-CNK** is verified using *in situ* UV-Vis-NIR spectroscopy, Raman spectroscopy, and MALDI-TOF mass spectrometry, supported by quantum chemical calculations. Mesityl substitution at the high-spin positions imparts moderate kinetic stability, resulting in a half-life ($t_{1/2}$) of 59 minutes under ambient conditions. Continuous-wave EPR analysis confirms the presence of unpaired electrons with a *g*-value of 2.0026. These results introduce a novel persistent concealed non-Kekulé NG, offering valuable insights for the design of CNK structural motifs having antiferromagnetic unpaired spins, with implications in the field of spintronics. Our ongoing work focuses on next-generation derivatives of **c-CNK** with enhanced kinetic stability through steric modifications, which will enable further exploration of their properties.

## Author contributions

All authors have given approval to the final version of the manuscript. MI and LY contributed equally to this work.

## Data availability

The data supporting this article have been included as part of the ESI.† The crystallographic data for **2H-c-CNK** have been deposited at the CCDC under 2390595.†

## Conflicts of interest

There are no conflicts to declare.

## Acknowledgements

This research was financially supported by the EU Graphene Flagship (Graphene Core 3, 881603), EIC-2022-Pathfinder Open (ATYPIQUAL, 101099098), the Center for Advancing Electronics Dresden (cfaed), H2020-EU.1.2.2.-FET Proactive Grant (LIGHT-CAP, 101017821) and the DFG-SNSF Joint Switzerland-German Research Project (EnhanTopo, 429265950). The authors gratefully acknowledge the GWK support for funding this project by providing computing time through the Center for Information Services and HPC (ZIH) at TU Dresden. MI is thankful to the Alexander von Humboldt Foundation for generous postdoctoral fellowship support.

## References

1 W. Zeng and J. Wu, Open-Shell Graphene Fragments, *Chem*, 2021, **7**(2), 358–386.
2 J. Liu and X. Feng, Synthetic Tailoring of Graphene Nanostructures with Zigzag-Edged Topologies: Progress and Perspectives, *Angew. Chem., Int. Ed.*, 2020, **59**(52), 23386–23401.
3 D. G. de Oteyza and T. Frederiksen, Carbon-Based Nanostructures as a Versatile Platform for Tunable π-Magnetism, *J. Phys.: Condens. Matter*, 2022, **34**(44), 443001.
4 S. Song, J. Su, M. Telychko, J. Li, G. Li, Y. Li, C. Su, J. Wu and J. Lu, On-Surface Synthesis of Graphene Nanostructures with π-Magnetism, *Chem. Soc. Rev.*, 2021, **50**(5), 3238–3262.

5 T. Kubo, Phenalenyl-Based Open-Shell Polycyclic Aromatic Hydrocarbons, *Chem. Rec.*, 2015, **15**(1), 218–232.
6 H. Miyoshi, S. Nobusue, A. Shimizu and Y. Tobe, Non-Alternant Non-Benzenoid Kekulenes: The Birth of a New Kekulene Family, *Chem. Soc. Rev.*, 2015, **44**(18), 6560–6577.
7 Y. Morita, S. Suzuki, K. Sato and T. Takui, Synthetic Organic Spin Chemistry for Structurally Well-Defined Open-Shell Graphene Fragments, *Nat. Chem.*, 2011, **3**(3), 197–204.
8 F. Lombardi, A. Lodi, J. Ma, J. Liu, M. Slota, A. Narita, W. K. Myers, K. Müllen, X. Feng and L. Bogani, Quantum Units from the Topological Engineering of Molecular Graphenoids, *Science*, 2019, **366**(6469), 1107–1110.
9 T. Kubo, Syntheses and Properties of Open-Shell π-Conjugated Molecules, *Bull. Chem. Soc. Jpn.*, 2021, **94**(9), 2235–2244.
10 S. K. Pal, M. E. Itkis, F. S. Tham, R. W. Reed, R. T. Okley and R. C. Haddon, Resonating Valence-Bond Ground State in a Phenalenyl-Based Neutral Radical Conductor, *Science*, 2005, **309**(5732), 281–284.
11 I. Žutić, J. Fabian and S. Das Sarma, Spintronics: Fundamentals and Applications, *Rev. Mod. Phys.*, 2004, **76**(2), 323–410.
12 D. Gatteschi, L. Bogani, A. Cornia, M. Mannini, L. Sorace and R. Sessoli, Molecular Magnetism, Status and Perspectives, *Solid State Sci.*, 2008, **10**(12), 1701–1709.
13 K. Goto, T. Kubo, K. Yamamoto, K. Nakasuji, K. Sato, D. Shiomi, T. Takui, M. Kubota and T. Kobayashi, A Stable Neutral Hydrocarbon Radical: Synthesis, Crystal Structure, and Physical Properties, *J. Am. Chem. Soc.*, 1999, **778**(6), 1619–1620.
14 Y. Li, K.-W. Huang, Z. Sun, R. D. Webster, Z. Zeng, W. Zeng, C. Chi, K. Furukawa and J. Wu, A Kinetically Blocked 1,14:11,12-Dibenzopentacene: A Persistent Triplet Diradical of a Non-Kekulé Polycyclic Benzenoid Hydrocarbon, *Chem. Sci.*, 2014, **5**(5), 1908–1914.
15 S. Arikawa, A. Shimizu, D. Shiomi, K. Sato and R. Shintani, Synthesis and Isolation of a Kinetically Stabilized Crystalline Triangulene, *J. Am. Chem. Soc.*, 2021, **143**(46), 19599–19605.
16 L. Valenta, M. Mayländer, P. Kappeler, O. Blacque, T. Šolomek, S. Richert and M. Juríček, Trimesityltriangulene: A Persistent Derivative of Clar's Hydrocarbon, *Chem. Commun.*, 2022, **58**(18), 3019–3022.
17 X. Guo, F. Zhang, J. Brunvoll, B. N. Cyvin and S. J. Cyvin, Concealed Non-Kekuléan Benzenoids, *J. Chem. Inf. Comput. Sci.*, 1995, **35**(2), 226–232.
18 R. Ortiz, R. A. Boto, M. Melle-franco and J. Fernández-Rossie, Exchange Rules for Diradical π-Conjugated Hydrocarbons, *Nano Lett.*, 2019, **19**(9), 5991–5997.
19 S. Gil-Guerrero, M. Melle-Franco, Á. Peña-Gallego and M. Mandado, Clar Goblet and Aromaticity Driven Multiradical Nanographenes, *Chem. – Eur. J.*, 2020, **26**(68), 16138–16143.
20 S. J. Cyvin, J. Brunvoll and B. N. Cyvin, The Hunt for Concealed Non-Kekuléan Polyhexes, *J. Math. Chem.*, 1990, **4**(1), 47–54.
21 E. Clar and C. C. Mackay, Circobiphenyl and the Attempted Synthesis of 1:14, 3:4, 7:8, 10:11-Tetrabenzoperopyrene, *Tetrahedron*, 1972, **28**(24), 6041–6047.
22 S. Mishra, D. Beyer, K. Eimre, S. Kezilebieke, R. Berger, O. Gröning, C. A. Pignedoli, K. Müllen, P. Liljeroth, P. Ruffieux, X. Feng and R. Fasel, Topological Frustration Induces Unconventional Magnetism in a Nanographene, *Nat. Nanotechnol.*, 2020, **15**(1), 22–28.
23 E. Turco, A. Bernhardt, N. Krane, L. Valenta, R. Fasel, M. Juríček and P. Ruffieux, Observation of the Magnetic Ground State of the Two Smallest Triangular Nanographenes, *JACS Au*, 2023, **3**(5), 1358–1364.
24 X. Su, C. Li, Q. Du, K. Tao, S. Wang and P. Yu, Atomically Precise Synthesis and Characterization of Heptauthrene with Triplet Ground State, *Nano Lett.*, 2020, **20**(9), 6859–6864.
25 S. Song, A. Pinar Solé, A. Matěj, G. Li, O. Stetsovych, D. Soler, H. Yang, M. Telychko, J. Li, M. Kumar, Q. Chen, S. Edalatmanesh, J. Brabec, L. Veis, J. Wu, P. Jelinek and J. Lu, Highly Entangled Polyradical Nanographene with Coexisting Strong Correlation and Topological Frustration, *Nat. Chem.*, 2024, **16**(6), 938–944.
26 N. Pavliček, A. Mistry, Z. Majzik, N. Moll, G. Meyer, D. J. Fox and L. Gross, Synthesis and Characterization of Triangulene, *Nat. Nanotechnol.*, 2017, **12**(4), 308–311.
27 S. Mishra, D. Beyer, K. Eimre, J. Liu, R. Berger, O. Gröning, C. A. Pignedoli, K. Müllen, R. Fasel, X. Feng and P. Ruffieux, Synthesis and Characterization of π-Extended Triangulene, *J. Am. Chem. Soc.*, 2019, **141**(27), 10621–10625.
28 J. Su, M. Telychko, P. Hu, G. Macam, P. Mutombo, H. Zhang, Y. Bao, F. Cheng, Z.-Q. Huang, Z. Qiu, S. J. R. Tan, H. Lin, P. Jelínek, F.-C. Chuang, J. Wu and J. Lu, Atomically Precise Bottom-up Synthesis of π-Extended [5]Triangulene, *Sci. Adv.*, 2019, **5**, 4–10.
29 F. Wu, J. Ma, F. Lombardi, Y. Fu, F. Liu, Z. Huang, R. Liu, H. Komber, D. I. Alexandropoulos, E. Dmitrieva, T. G. Lohr, N. Israel, A. A. Popov, J. Liu, L. Bogani and X. Feng, Benzo-Extended Cyclohepta[Def]Fluorene Derivatives with Very Low-Lying Triplet States, *Angew. Chem., Int. Ed.*, 2022, **61**(23), e202202170.
30 K. Sahara, M. Abe, H. Zipse and T. Kubo, Duality of Reactivity of a Biradicaloid Compound with an o-Quinodimethane Scaffold, *J. Am. Chem. Soc.*, 2020, **142**(11), 5408–5418.
31 M. R. Ajayakumar, J. Ma, A. Lucotti, K. S. Schellhammer, G. Serra, E. Dmitrieva, M. Rosenkranz, H. Komber, J. Liu, F. Ortmann, M. Tommasini and X. Feng, Persistent Peri-Heptacene: Synthesis and *In situ* Characterization, *Angew. Chem., Int. Ed.*, 2021, **60**(25), 13853–13858.
32 Y. Li, W.-K. Heng, B. S. Lee, N. Aratani, J. L. Zafra, N. Bao, R. Lee, Y. M. Sung, Z. Sun, K.-W. Huang, R. D. Webster, J. T. López Navarrete, D. Kim, A. Osuka, J. Casado, J. Ding and J. Wu, Kinetically Blocked Stable Heptazethrene and Octazethrene: Closed-Shell or Open-Shell in the Ground State?, *J. Am. Chem. Soc.*, 2012, **134**(36), 14913–14922.